BBA - Biomembranes 1859 (2017) 2106–2112

Contents lists available at ScienceDirect

BBA - Biomembranes

journal homepage: www.elsevier.com/locate/bbamem

Binding of a type 1 RIP and of its chimeric variant to phospholipid bilayers: evidence for a link between cytotoxicity and protein/membrane interactions

Elio Pizzo[a,1], Rosario Oliva[b,1], Rita Morra[b], Andrea Bosso[a], Sara Ragucci[c], Luigi Petraccone[b], Pompea Del Vecchio[b,*], Antimo Di Maro[c,*]

[a] Department of Biology, University of Naples 'Federico II', Via Cintia, I-80126 Napoli, Italy
[b] Department of Chemical Sciences, University of Naples 'Federico II', Via Cintia, I-80126 Napoli, Italy
[c] Department of Environmental, Biological and Pharmaceutical Sciences and Technologies, University of Campania 'Luigi Vanvitelli', I-81100 Caserta, Italy

ARTICLE INFO

Keywords:
Bio-conjugates
Calorimetry
Membrane interactions
Liposomes
Ribosome-inactivating proteins
Protease inhibitors

ABSTRACT

Ribosome-inactivating proteins (RIPs) are enzymes, almost all identified in plants, able to kill cells by depurination of rRNAs. Recently, in order to improve resistance to proteolysis of a type 1 RIP (PD-L4), we produced a recombinant chimera combining it with a wheat protease inhibitor (WSCI). Resulting chimeric construct, named PD-L4UWSCI, in addition to present the functions of the two domains, shows also an enhanced cytotoxic action on murine cancer cells when compared to PD-L4. Since different ways of interaction of proteins with membranes imply different resulting effects on cells, in this study we investigate conformational stability of PD-L4 and PD-L4UWSCI and their interaction with membrane models (liposomes). Circular dichroism analysis and differential scanning calorimetry measurements indicate that PD-L4 and PD-L4UWSCI present high and similar conformational stability, whereas analysis of their binding to liposomes, obtained by isothermal titration calorimetry and differential scanning calorimetry, clearly indicate that chimera is able to interact with biomembranes more effectively.

Overall, our data point out that WSCI domain, probably because of its flexibility in solution, enhances the chimeric protein interaction with membrane lipid surfaces without however destabilizing the overall protein structure. Analysis of interactions between RIPs or RIP based conjugates and lipid surfaces could provide novel insights in the search of more effective selective membrane therapeutics.

1. Introduction

The cancer is one of the leading causes of death in the world, in fact more than 14% of human deaths are imputable to this disease [1,2]. In this framework, the global scientific research is focused on developing therapeutic strategies to obtain a successful treatment of cancer, despite the serious difficulties due to the emergence of resistance, which often leads to the development of new abnormal cells with aggressive characteristics [3]. During the years, cancer treatment has pursued various strategies able to specifically destroy cancer cells such as chemotherapy [4], immunotherapy [5] radiation therapy [6] and approaches by using immunotoxins [3,7] or treatments with hormones [8,9].

Among these strategies, the development of immunoconjugates involves the use of chimeric molecules obtained combining antibody or its portion and specific toxins that rely on intracellular toxin action to kill target cells [10]. This approach is based on antibody specificity to select target on cancerous cells, thus allowing an effective toxin delivery specifically on abnormal cells [11]. Generally, the toxin belong to enzymes, such as ribonucleases (e.g. RNase 1 [12] and α-sarcin [13]), ADP-ribosyltransferases (e.g. diphtheria toxin and exotoxin A from *Pseudomonas* [14,15]) or several *N*-glycosilases (e.g. ribosome inactivating proteins - RIPs) [16,17]. In all cases, many factors determine sensitivity or resistances to the immunoconjugates such as access to target cells, binding to target cells, cell entry, routing [18] or proteolysis susceptibility. The latter statement is well documented by several authors that described studies of RIPs based immunotoxins [19,20].

RIP enzymes (EC: 3.2.2.22) are a family of well-characterized toxins, which possess N-β-glycosilase activity able to cleave a specific

Abbreviations: (RIPs), Ribosome-inactivating proteins; POPC, 1-palmitoyl-2-oleoyl-sn-glycero-3-phosphocholine; POPG, 1-palmitoyl-2-oleoyl-sn-glycero-3-phosphoglycerol; DPPC, 1,2-dipalmitoyl-sn-glycero-3-phosphocholine; DPPG, 1,2-dipalmitoyl-sn-glycero-3-phosphoglycerol; MLVs, Multi-Lamellar Vesicles; SUVs, Small Uni-Lamellar vesicles; LUVs, Large Uni-Lamellar vesicles

* Corresponding authors.
E-mail addresses: pompea.delvecchio@unina.it (P. Del Vecchio), antimo.dimaro@unicampania.it (A. Di Maro).
[1] These authors have contributed equally to this work.

http://dx.doi.org/10.1016/j.bbamem.2017.08.004
Received 20 June 2017; Received in revised form 28 July 2017; Accepted 4 August 2017
Available online 07 August 2017
0005-2736/ © 2017 Elsevier B.V. All rights reserved.

adenine residue from 28S rRNA in the exposed Sarcin/Ricin Loop (SRL) [21] and irreversibly to inhibit protein synthesis in eukaryotic cells [22]. RIPs are classified depending on if possess or not quaternary structure: type 1 basic proteins with N-glycosidase activity (A chain) without lectin-like chain (B chain) and type 2 chain with a lectin-like B chain linked to A chain by a disulphide bond [22,23]. Most of them are produced by plants [24] and are thought to represent a defence mechanism against viral or parasitic attackers [25–27].

Most effective bioactive conjugated are based on chemical linkage between RIP and antibodies, lectins, growth factors or nanoparticles [16,27]. However, action of RIPs, alone or as conjugates is closer correlated to its intracellular routing [28,29].

An increasing number of reports indicate RIPs as effective moiety in the construction of conjugates for developing selective antiviral and anticancer agents [17]. Cytotoxicity of RIPs, alone or as conjugates, is due not only to their enzymatic activity but also to their cellular routing. This is also confirmed by the existence of non-toxic RIPs (e.g. from *Sambucus*), that although retaining their N-glycosidase activity, are unable to kill the cells because they are involved in different intracellular routing with respect to toxic RIPs [30].

Our research group, in order to develop a new generation of RIP based chimeric conjugates less susceptible to proteolytic degradation during their intracellular routing, have designed a novel specific chimeric toxin [31]. It is composed, as below schematically reported, by a type 1 RIP from *Phytolacca dioica* L. (PD-L4; UniProt code: P84854) [32] and a protease inhibitor from endosperm of hexaploid seeds of *Triticum aestivum* L. (WSCI; UniProt code: P82977) [33].

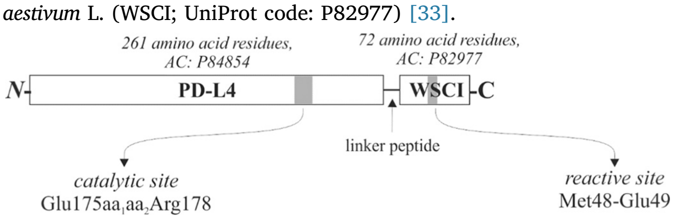

The chimeric protein, named PD-L4UWSCI, consists of two domains: an amino-terminal PD-L4 domain fused to a C-terminal WSCI domain. Catalytic site of PD-L4 and reactive site of WSCI are indicated in grey. The linker peptide is composed by residues **LEQASSYTAPQPQPG**. AC: UniProt (http://www.uniprot.org/) accession number.

This recombinant construct, hereafter PD-L4UWSCI, has proved to possess intact intrinsic activity of both domains (e.g. enzymatic activity and inhibitory properties) and at the same time it presented an enhanced intriguingly selective cytotoxicity on murine tumour cells [31]. Subsequently, in order to verify if this increased selective cytotoxicity could be due to the anti-chimotryptic inhibitory specificity mediated by WSCI moiety, a mutant chimeric construct was produced, in which inhibitory specificity was modified (anti-chimotryptic versus anti-tryptic), substituting two amino acid residues (325[P1] and 326[P1']) [34]. As reported in [34], mutated specificity of inhibition on WSCI domain, did not alter cytotoxicity of chimeric construct. This invalidate the hypothesis on a possible contribution of WSCI specificity to anti-tumour action of the chimeric construct but, at the same time it is conceivable that WSCI could contribute to the observed chimeric protein cytotoxic activity on malignant cells by altering structural/energetic properties of the protein and of its interaction capability with other biomolecules. Based on these considerations, it is plausible to imagine different ways of interaction between PD-L4 or PD-L4UWSCI, with membrane phospholipid bilayers; besides, it should be noted that normal and cancerous cells present different lipid compositions, which can play a key role in cell/macromolecules interactions [35–37].

In the present work, we characterized the conformational stability (by thermal and GuHCl-induced unfolding measurements) as well as the interaction with cancer cell membrane models, as of recombinant protein PD-L4 compared to the construct PD-L4UWSCI. Our data reveals that WSCI has a marginal effect on the protein stability but significantly increases the protein ability to interact with lipid bilayers and to modify the membrane biophysical properties.

2. Material and methods

2.1. Materials

Expression vector pET 22b($^+$) and *E. coli* strain BL21 (DE3) were from AMS Biotechnology (Lugano, Switzerland). Other reagents for DNA manipulation and rabbit reticulocyte lysate were from Promega Biotech (Milan, Italy) or were described elsewhere [31,34]. Trypsin, alpha-chymotrypsin, protease substrates (BTEE, NBA and TAME), antibiotics, DEPC, and reagents for cell culture were purchased from Sigma Aldrich (Milan, Italy). Bicinchoninic acid (BCA) kit was purchased from Pierce (Rockford, IL, USA).

2.2. Expression and purification of recombinant chimera or PD-L4

Expression, refolding, and purification of recombinant proteins (rPD-L4 or rPD-L4UWSCI) were performed according to Del Vecchio Blanco et al. [38] (**Fig. S1**). Each step of the expression and purification procedure was monitored by SDS-PAGE analyses. The eluted protein from the cation exchange chromatography on SOURCE 15S 4.6/100 PE column (1.7 mL) using Akta purifier system (GE Healthcare, Milan, Italy) was collected, dialyzed, and kept frozen until use.

2.3. Enzymatic assays

28S rRNA N-glycosidase activity was assayed as previously described [39] by incubating rabbit reticulocyte lysate (80 μL) with 2 μg of PD-L4 or PD-L4UWSCI. α-chymotryptic and anti-α-chymotryptic activities, as well as tryptic and anti-tryptic activities were determined as previously reported [33] by using BTEE and TAME as synthetic substrates.

2.4. Liposome preparation

Appropriate amounts of lipids were weighed and dissolved in chloroform/methanol (2/1 v/v). A thin film of the lipids was produced by evaporating the solvent with dry nitrogen gas, and placed in a vacuum overnight. The sample was then hydrated with a definite amount of 20 mM sodium phosphate buffer at pH 7.4 and vortexed obtaining a suspension of multilamellar vesicles (MLVs). Vesicles composed by DPPC/DPPG (80/20 mol%) were used for DSC measurements while vesicles composed by POPC/POPG (80/20 mol%) were used for ITC binding measurements. In the latter case, large unilamellar vesicles, (LUVs) were prepared by the extrusion methods using a Mini-Extruder (Avanti Polar Lipid Inc.). The liposome suspensions were extruded through 100 nm polycarbonate filters.

2.5. Circular dichroism

CD spectra in the far UV-region (190–250 nm) were recorded on a Jasco J-715 spectropolarimeter under constant nitrogen flow, equipped with a Peltier type temperature control system (Model PTC-348WI). The spectra were recorded in a 0.1 cm cell, with a 4 s response time, 2 nm bandwidth and 20 nm/min scan rate, averaged over three scans, and finally corrected for the buffer signal. Cell cuvette thickness and protein concentration were chosen in a way that the maximum high-tension voltage of the photomultiplier was not exceeding 600 V at the lowest wavelength of 190 nm. Mean residue ellipticity values (MRE), [θ] in deg cm^2 dmol^{-1}, were calculated by the following relation: $[\theta] = [\theta]_{obs}\ M_w / n\ 10 \times l \times C$, where θ is the measured ellipticity (millidegrees), M_w is the molecular mass of the protein in Da, n is the number of amino acid residues, C is the protein concentration in mg/mL, and l is the path length in cm. Typically, we used protein concentrations between 0.1 and 0.2 mg/mL. CD spectra of the proteins in the presence of LUVs were recorded in the same experimental conditions as in the buffer. Samples of the proteins in the presence of vesicles were prepared by adding preformed vesicles in the protein solution at the desired lipid to peptide ratio. Spectra were recorded at fixed temperatures of 25 °C averaged, and corrected for the buffer baseline. An estimation of the secondary structure content was obtained from the spectra using DICHROWEB analysis webserver [40]. Thermal unfolding curves were recorded in the far-UV region at 222 nm, from 25 °C to 95 °C, every 0.5 °C with a scan rate of 1 °C min^{-1} at a protein concentration of 0.1 mg/mL. They were analysed assuming a two-state N ⇄ D unfolding mechanism [41]. The denaturant-induced unfolding was monitored by following changes in the CD signal at 222 nm of solutions containing an identical concentration of protein, which was previously incubated overnight at 4 °C with increasing concentration of GuHCl. The concentrations of denaturant stock solutions were derived from refractive index measurements. The CD spectra were recorded at different GuHCl concentration, using a 0.1 cm path length cell. The data were then analyzed in the assumption of a two-state N ⇄ D transition, by means of a linear extrapolation model (LEM) [42]. The standard denaturation Gibbs energy change is assumed to be a linear function of the denaturant concentration, [GuHCl] according to the equation $\Delta_dG = \Delta_dG(H_2O) - m\,[GuHCl]$, where $\Delta_dG(H_2O)$ is the value of Δ_dG in the absence of denaturant and m is a measure of the dependence of Δ_dG on denaturant concentration. Furthermore, $\Delta_dG(H_2O) = m\,[GuHCl]_{1/2}$, where $[GuHCl]_{1/2}$ is the midpoint of the denaturant-induced process. A nonlinear least squares regression was carried out to estimate the unknown parameters associated with the unfolding transition, using the Origin software package.

2.6. Differential scanning calorimetry

Calorimetric measurements were carried out by using a Nano-DSC (TA Instruments, USA) with capillary cells of 0.3 ml sensitive volume. A total pressure of 3.0 atm was applied with nitrogen gas to both cells during the temperature scanning. The excess molar heat capacity function, $< \Delta C_P >$, was obtained after a baseline subtraction, assuming that the baseline is given by the linear temperature dependence of the heat capacity of sample in the pre-transition temperature range. Buffer-buffer scans were recorded under the same conditions and subtracted from sample endotherms. Protein samples were prepared in the appropriate buffer solution with a concentration of about 0.5–0.8 mg mL^{-1} for all DSC experiments. A reheating run of the sample under identical conditions showed no endotherm indicating that the protein thermal denaturation was fully irreversible, thus preventing a complete characterization of the thermal denaturation.

MLVs of phospholipids DPPC/DPPG (80/20 mol%) were used for all DSC experiments. The lipid film was prepared as described, then hydrated using buffer solution, and vortexed to obtain a homogeneous dispersion. Samples of the vesicles in the presence of proteins were prepared by adding the protein solution to the preformed vesicles at ambient temperature. The samples were then equilibrate at 50 °C for 6 h before the DSC scans. A volume of 300 μL of sample (0.5 mM) was placed in the calorimetry vessel. Successive heating and cooling scans (at least 4) at scanning rate of 1 °C min^{-1} were performed for each sample over the temperature range of 25–55 °C while the last heating up to 95 °C. Successive heating and cooling scans in the 25–55 °C range were superimposed, to get insight into the reversibility of the process. DSC data were analyzed by means of the Nano-Analyze software supplied with the instrument and plotted using the Origin software package.

2.7. Isothermal titration calorimetry

ITC measurements were performed using a Nano-ITC III (TA instruments, New Castle, DE, USA) at 25 °C. The protein solution (15 μM) was injected in the calorimetric vessel (1 mL) containing LUVs of POPC/POPG (80/20 mol%) lipid mixture (7 mM total lipid concentration). A volume of 100 μL of the protein solution was injected in aliquots of 10 μL with 400 s intervals between the individual injections. Under these conditions, the lipid is much in excess over the protein solution during the whole titration experiment, and the injected protein is completely bound to the membrane surface [43]. Each injection should produce the same heat providing the binding enthalpy when divided by the mole of protein. A control experiment, in which the protein solution was injected into the cell containing the buffer, was performed and the change of heat transfer per injection was subtracted. The obtained data were analyzed using the Nano-Analyze software supplied with the instrument and plotted using the Origin software package.

3. Results and discussion

3.1. Protein thermodynamic stability

To date no evidence has been reported on the physicochemical properties of PD-L4. The study of thermodynamic properties of PD-L4 protein and of its chimeric construct aims to elucidate the role of WSCI domain in the conformational stability of the protein. Thermodynamic investigations were conducted by thermal and GuHCl-induced unfolding using differential scanning calorimetry (DSC) and circular dichroism (CD) measurements.

3.1.1. Thermal unfolding

Far-UV CD spectra of the proteins are reported in Fig. 1. CD spectrum of rPD-L4 indicates that the protein is well folded in solution; indeed the analysis of the spectrum by means of DichroWeb [44] gives values of 34% α-helix and 19% β-sheet in very close agreement with structural crystallographic data [45]. The analysis of CD spectrum of rPD-L4UWSCI gives values of 28% α-helix and 17% β-sheet showing a reduction in the content in the secondary structure, thus suggesting a presumably almost total absence of a defined conformation in the WSCI domain [46]. Thermal denaturation curves, obtained by recording changes in CD signal at 222 nm, show a sigmoidal behaviour with a T_d of 83.5 °C and 82 °C for rPD-L4 and rPD-L4UWSCI, respectively (inset Fig. 2). Thermal unfolding of rPD-L4 and rPD-L4UWSCI was monitored also by DSC measurements. DSC is a very suitable technique to study and quantify the thermodynamic parameters relative to non-covalent bond formation in proteins. This calorimetric technique provides a direct estimation of protein denaturation parameters as it gives information on each process occurring along with heat transfer [47]. Fig. 2 shows the DSC profiles obtained for rPD-L4 and rPD-L4UWSCI proteins in solution. All the investigated samples showed irreversible DSC profiles as no detectable DSC peak was observed on reheating the

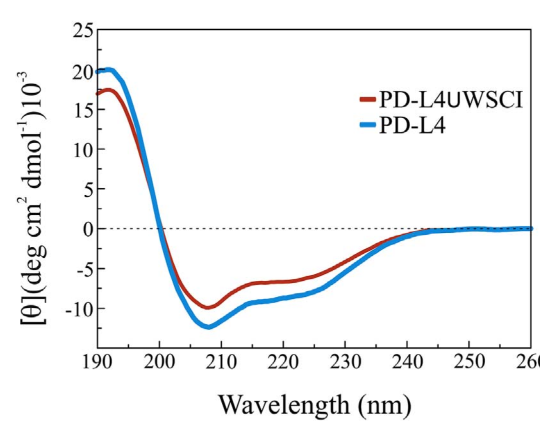

Fig. 1. Far-UV CD spectra of rPD-L4 (blue line) and PD-L4UWSCI (red line) in a 20 mM sodium phosphate buffer solution, pH 7.4 and 25 °C.

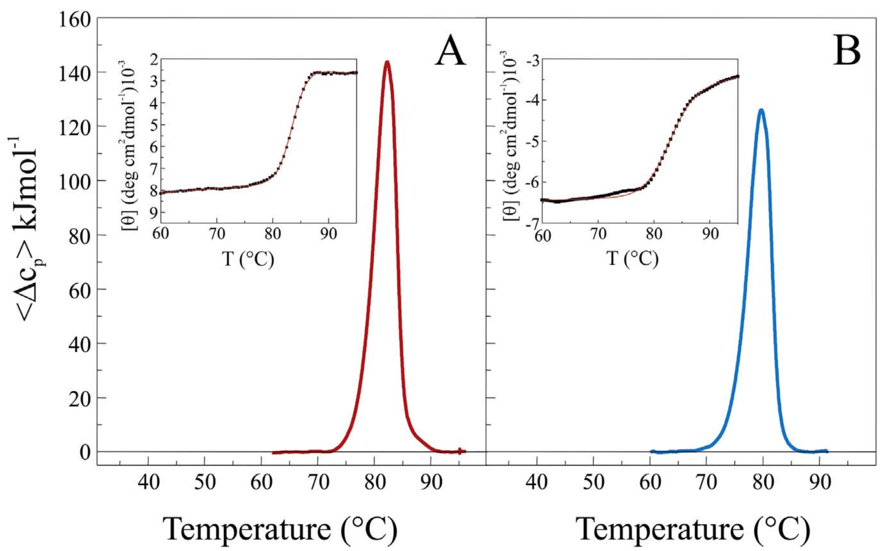

Fig. 2. Normalized DSC profiles of (A) rPD-L4 and (B) PD-L4UWSCI in 20 mM phosphate buffer, pH 7.4. The insets show the CD thermal unfolding curve of (A) rPD-L4 and (B) PD-L4UWSCI. The red line represents the best fit of experimental data obtained using a two state model for denaturation.

Table 1
Thermodynamic parameters for the thermal (*) and GuHCl-induced unfolding (**) of rPD-L4 and rPD-L4UWSCI.

	T_d (°C)	$\Delta_d H_{cal}$ (kJ mol^{-1})	$[GuHCl]_{1/2}$ (M)	$\Delta_d G_{H2O}$ (kJ mol^{-1})	m (kJ mol^{-1}M^{-1})
rPD-L4	82.3	740	3.6	48	12.0
rPD-L4UWSCI	79.7	670	3.3	43	13.0

* DSC measurements. ** CD measurements. Each number represents the value averaged over at least three measurements. Errors for T_d, enthalpy and Gibbs energy are within 0.5 °C, 5% and 10%, respectively.

samples previously heated up to 90 °C. The irreversibility of thermal denaturation prevented a complete thermodynamic characterization. The values of denaturation temperature and enthalpy change were 82.3 ± 0.5 °C and 740 ± 36 kJ mol^{-1} for rPD-L4 and 79.7 °C and 670 ± 33 kJ mol^{-1} for rPD-L4UWSCI (Table 1). These data reveal that both proteins possess a high thermal stability whereas the lower enthalpy changes observed for rPD-L4UWSCI denaturation is consistent with the WSCI domain, the latter with a coiled conformation in solution, as previously reported [46].

3.1.2. Denaturant-induced unfolding

The well-defined CD spectra recorded for both proteins indicate that far-UV CD signal is appropriate as a probe to monitor denaturant induced changes in the secondary structure of the proteins. In Fig. 3, the GuHCl-induced denaturation curves for rPD-L4 and rPD-L4UWSCI, obtained by recording the molar ellipticity at 222 nm, are reported. The GuHCl-induced unfolding of both proteins was reversible since the renaturation of completely unfolding samples, upon suitable dilution, showed a full recovery of the CD signal (**see Fig. S2**). A thermodynamic analysis was performed assuming a reversible two state N ⇄ D denaturation process. The obtained results, summarized in Table 1, indicated that: i) the GuHCl-induced unfolding of rPD-L4 and rPD-L4UWSCI can be described by a N ⇄ D reversible process, as a simple sigmoidal curve was obtained for both proteins; ii) both proteins possess high resistance against GuHCl denaturing action showing high $[GuHCl]_{1/2}$ values of 3.6 M and 3.3 M, respectively. Further, the $\Delta_d G$ (H_2O) and m values calculated from the analysis were found comparable within the experimental errors (Table 1) suggesting that the rPD-L4 protein and the chimeric construct rPD-L4UWSCI, possess high and similar conformational stability. This is not surprising as the WSCI domain is probably unordered in solution and does not contribute significantly to the protein stability. The overall results on thermal and GuHCl-induced unfolding showed that both proteins have a high and very similar conformational stability.

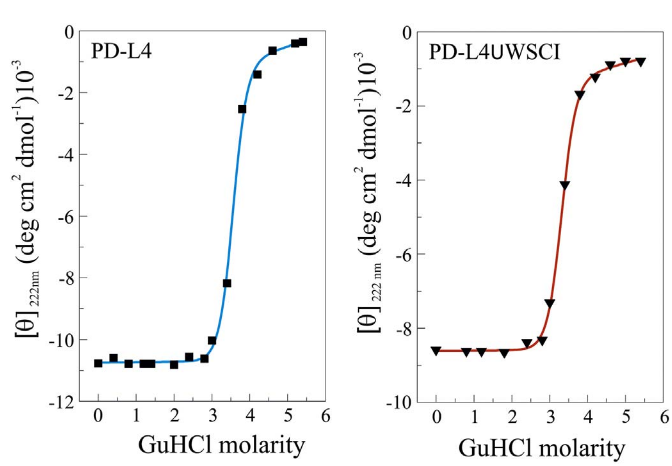

Fig. 3. GuHCl-induced unfolding curves of rPD-L4 (A) and PD-L4UWSCI (B) in 20 mM buffer at pH 7.4, recorded by following changes in the CD signal at 222 nm, at 25 °C. The solid lines represent the best fit of experimental points obtained with the two-state denaturation process analysis.

3.2. Protein/liposome interaction

The interaction between proteins and bio-membranes could be a key factor in determining their biological activity. We, thus, decided to explore the interaction of PD-L4 and its chimeric construct with bio-membranes by using negative liposomes (see Material and methods) as a model of cancer cell membranes. The thermodynamics of the protein-membrane interaction were determined by means of Isothermal Titration Calorimetry (ITC) measurements whereas the effect of the protein binding on the thermotropic properties of the membrane was monitored by means of Differential Scanning Calorimetry (DSC) measurements.

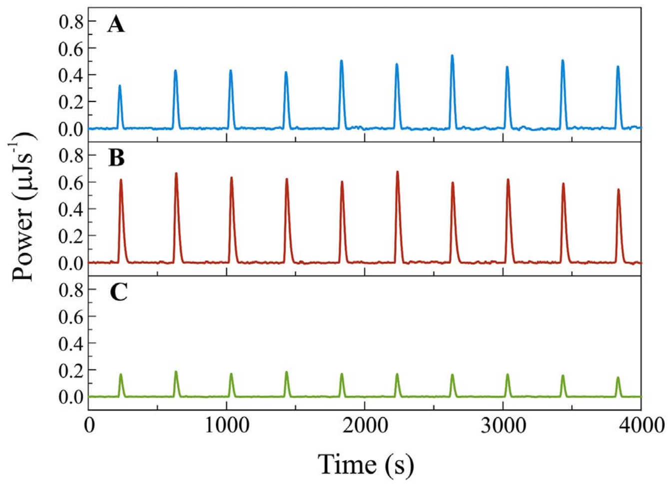

Fig. 4. ITC traces obtained from the titration of POPC/POPG (8/2 mol/mol) vesicles (total lipid concentration of 7 mM) with a solution of rPD-L4 (A) and PD-L4UWSCI (B). (C) ITC trace obtained from the dilution experiment of rPD-L4 against buffer solution. The experiments were carried out at the protein concentration of 15 μM in 20 mM phosphate buffer, pH 7.4 at 25 °C.

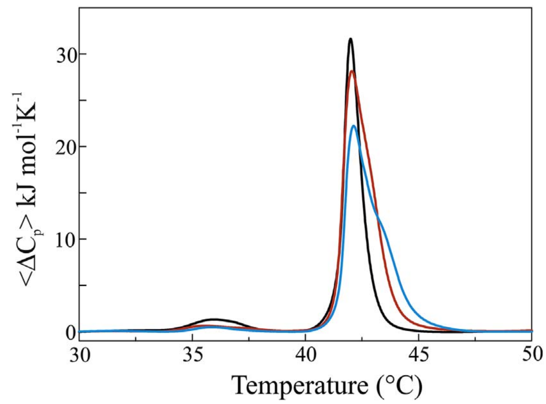

Fig. 5. Normalized DSC profiles for the gel to liquid phase transition of DPPC/DPPG multilamellar vesicles in the absence (black) and in the presence of rPD-L4 (red) and of PD-L4UWSCI (blue) at the lipid-to-protein molar ratio of 50. All the experiments were carried out in 20 mM phosphate buffer, pH 7.4.

Table 2
Thermodynamic parameters obtained by means of DSC for the gel to liquid phase transition of DPPC/DPPG (80/20 % mol) liposomes.

	ΔH_p (kJ mol^{-1})[a]	T_p (°C)	ΔH_m (kJ mol^{-1})[a]	T_m (°C)
DPPC/DPPG	3.0 ± 0.2	36.0 ± 0.1	34.4 ± 1.7	42.0 ± 0.1
+ rPD-L4	1.5 ± 0.1	35.7 ± 0.1	43.1 ± 2.2	42.1 ± 0.1
+ rPD-L4UWSCI			40.1 ± 2.0	42.9 ± 0.1

Each number represents the value averaged over at least three measurements.
[a] The enthalpy changes are normalized against total lipid moles.

3.2.1. *The protein point of view: isothermal titration calorimetry (ITC)*

In order to investigate the interaction of rPD-L4 and rPD-L4UWSCI with membranes, we performed ITC measurements of the proteins using, as model membranes, liposomes composed of POPC/POPG lipids (80/20 mol%). The enthalpy of the binding process was directly measured by injecting a dilute protein solution into the ITC cell containing concentrated vesicles. Under these conditions, the lipid is much in excess over the protein during the whole titration experiment, and the injected protein is completely bound to the vesicles surface. In Fig. 4 are reported the ITC traces obtained for the rPD-L4 (panel A) and rPD-L4UWSCI (panel B) into the vesicles titration compared with the ITC trace obtained for the buffer solution into the vesicles titration (panel C). As expected, due to the high lipid to protein ratio (ranged between 40,000 and 4000), each injection produced the same heat effect. Analysis of the ITC traces obtained by the titration of rPD-L4 into the vesicles provides a negative value of association enthalpy of -58.0 ± 8.6 kJ mol^{-1}, showing that a favourable enthalpy contribution in the protein-liposome interaction occurs. The titration of rPD-L4UWSCI into the vesicles gives a negative value of the binding enthalpy of -98.0 ± 6.4 kJ mol^{-1}, showing that the enthalpy contribution to the interaction is almost twice with respect to that of rPD-L4. This higher value of the binding enthalpy of rPD-L4UWSCI could arise from different contributions as the formation of additional interactions between the WSCI domain and the membrane as well as from other phenomena as WSCI folding upon binding or liposomes fusion. To verify the relevance of these last two phenomena we performed additional CD and DLS experiments on the protein-liposome complex. CD experiments (Fig. S3) did not show significant protein conformational changes upon binding to the membrane and DLS measurements, performed before and after the ITC measurements, and revealed that the size (diameter ~125 nm) and integrity of liposomes does not change upon proteins binding (Fig. S4). Based on these observations, we can attribute the higher enthalpy values observed almost entirely to the ability of the WSCI domain to establish additional interaction with the lipid bilayers.

3.2.2. *The liposome point of view: differential scanning calorimetry (DSC)*

DSC experiments were performed to shed light on the effects of rPD-L4 and rPD-L4UWSCI on the thermotropic phase transition of liposomes. Vesicles composed by DPPC/DPPG were used to replace POPC/POPG lipid, as they show the main phase transition in a temperature range suitable for DSC measurements and retain the same heads groups of choline (PC) and glycerol (PG). DSC profile of DPPC/DPPG vesicles (Fig. 5 and Table 2) shows a pre-transition centred at 36.0 °C with a transition enthalpy of 3 kJ mol^{-1} and a main gel to liquid phase transition at 42.0 °C with an enthalpy change of 34.4 kJ mol^{-1}.

The addition of rPD-L4 or rPD-L4UWSCI markedly changed the DSC profiles of the DPPC/DPPG. Particularly, in the presence of rPDL4 (Fig. 5), the enthalpy of the pre-transition peak decreased of about 1.5 kJ mol^{-1}, whereas the main transition temperature remained almost unaltered but with the appearance of a shoulder centred at higher temperature (~43 °C).

In the presence of rPD-L4UWSCI (Fig. 5), the pre-transition is almost abolished and the main peak clearly appears as composed of two overlapping transitions centred at 42.9 °C and 43.5 °C, suggesting the presence of multiple domains in the membrane. For both rPD-L4 and rPD-L4UWSCI a substantial increase of the transition enthalpy was observed suggesting that both the proteins do not penetrate into the bilayer but rather interact electrostatically on the surface [48]. However, the extent of membrane perturbation upon proteins binding is greater for rPD-L4UWSCI suggesting that the coiled conformation of WSCI domain, as well as its several positive charged residues, could play a key role in optimizing interaction of chimeric construct with the bilayer surface. Interestingly, when the DSC scan was lengthened up to 95 °C, the proteins denaturation peak appeared and showed T_d and ΔH_{cal} quite similar to the ones observed in absence of liposomes (**Fig. S5** and **Table S1**). This result clearly suggests that the overall proteins structure is not significant altered upon membrane interaction, further supporting the hypothesis of surface binding.

4. Conclusions and perspectives

RIPs are enzymes widely studied for their ability to kill cells by depurination of rRNAs [22,30]. Various reports highlight their possible use in biomedical applications in form of chimeric bioconjugates, in which peculiar additional domains make selective their actions against target cancer cells [17].

The study reported in this paper has been focused on a type 1 RIP (PD-L4) and on its chimeric conjugate PD-L4UWSCI, obtained by fusing the enzyme with a serine inhibitor protease (WSCI). The main aim of this study was to investigate, by a physical-chemical approach, possible structural/energetic contributions of WSCI to the enhanced toxic activity of PD-L4UWSCI since we recently reported [31,34] specificity inhibitory properties of this additional domain do not influence toxic activity of chimeric construct. On this regard, protein thermodynamic stability and protein/liposome interaction studies have been carried out on both proteins.

Conformational stability studies showed that both recombinant proteins possess a similar high thermal stability, although PD-L4UWSCI is slightly less stable likely due to WSCI domain that presents a coiled conformation in solution. A similar result has been obtained by GuHCl-induced unfolded investigations. These evidences suggest that the proteins cytotoxic activity differences cannot be ascribed to a different conformational stability.

Therefore, we investigated, by isothermal titration calorimetry, the interaction between the proteins and POPC/POPG liposomes mimicking the plasmatic membrane of cancer cells. ITC results show that both proteins are able to interact with the lipid bilayer. However, the greater binding enthalpy found for rPD-L4UWSCI suggests that the chimeric protein is able to form additional interactions, attributable to the WSCI domain, with the lipid bilayer. We further investigated by differential scanning calorimetry, the effect of the proteins binding on the membrane thermotropic properties. DSC results suggest that both proteins do not penetrate significantly into the membrane but rather they interact electrostatically on the membrane surface. Interestingly, the extent of membrane perturbation upon protein binding was more marked for the chimeric protein corroborating our idea that the presence of WSCI domain plays a key role in optimizing its interaction with the bilayer surface. Altogether, our results suggest that WSCI play a key role in optimising the PD-L4UWSCI interaction with the cell membrane in comparison with PD-L4. This improved protein-membrane interaction could be a key factor in explaining its higher toxic activity.

Transparency Document

The Transparency document associated with this article can be found, in online version.

Acknowledgments

This study is the result of the dedication of all the participants due to the absence of dedicated funds and due to the chronic difficulties affecting the Italian scientific community. However, this work has been supported by the University of Campania 'Luigi Vanvitelli' and University of Naples 'Federico II'.

Appendix A. Supplementary data

Supplementary data to this article can be found online at http://dx.doi.org/10.1016/j.bbamem.2017.08.004.

References

[1] National_Cancer_Institute, What Is Cancer? (2015).
[2] A. Jemal, F. Bray, M.M. Center, J. Ferlay, E. Ward, D. Forman, Global cancer statistics, CA Cancer J. Clin. 61 (2011) 69–90.
[3] S. Gadadhar, A.A. Karande, Targeted cancer therapy: history and development of immunotoxins, in: R.S. Verma, B. Bonavida (Eds.), Resistance to Immunotoxins in Cancer Therapy, Springer International Publishing, Heidelberg (Germany), 2015, pp. 33–56.
[4] M.J. Lind, Principles of cytotoxic chemotherapy, Medicine 36 (2008) 19–23.
[5] T.A. Waldmann, Immunotherapy: past, present and future, Nat. Med. 9 (2003) 269–277.
[6] G.D.D. Jones, P. Symonds, Molecular, cellular and tissue effects of radiotherapy, in: R.P. Symonds, C. Deehan, C. Meredith, J.A. Mills (Eds.), Walter and Miller's Textbook of Radiotherapy: Radiation Physics, Therapy and Oncology, Churchill Livingstone - Elsevier, London, UK, 2012, pp. 279–292.
[7] I. Pastan, R. Hassan, D.J. FitzGerald, R.J. Kreitman, Immunotoxin treatment of cancer, Annu. Rev. Med. 58 (2007) 221–237.
[8] F. Labrie, Hormonal therapy of prostate cancer, Prog. Brain Res. 182 (2010) 321–341.
[9] G.Y. Locker, Hormonal therapy of breast cancer, Cancer Treat. Rev. 24 (1998) 221–240.
[10] A. Antignani, D. Fitzgerald, Immunotoxins: the role of the toxin, Toxins (Basel) 5 (2013) 1486–1502.
[11] A.A. Hertler, A.E. Frankel, Immunotoxins: a clinical review of their use in the treatment of malignancies, J. Clin. Oncol. 7 (1989) 1932–1942.
[12] T. Schirrmann, J. Krauss, M.A. Arndt, S.M. Rybak, S. Dubel, Targeted therapeutic RNases (ImmunoRNases), Expert. Opin. Biol. Ther. 9 (2009) 79–95.
[13] T.D. Jones, A.R. Hearn, R.G. Holgate, D. Kozub, M.H. Fogg, F.J. Carr, M.P. Baker, J. Lacadena, K.R. Gehlsen, A deimmunised form of the ribotoxin, alpha-sarcin, lacking $CD4^+$ T cell epitopes and its use as an immunotoxin warhead, Protein Eng. Des. Sel. (2016) 531–540.
[14] F. Shafiee, M. Rabbani, A. Jahanian-Najafabadi, Production and evaluation of cytotoxic effects of DT386-BR2 fusion protein as a novel anti-cancer agent, J. Microbiol. Methods 130 (2016) 100–105.
[15] M. Borowiec, M. Gorzkiewicz, J. Grzesik, A. Walczak-Drzewiecka, A. Salkowska, E. Rodakowska, K. Steczkiewicz, L. Rychlewski, J. Dastych, K. Ginalski, Towards engineering novel PE-based immunotoxins by targeting them to the nucleus, Toxins (Basel) 8 (2016) 321–340.
[16] E. Pizzo, A. Di Maro, A new age for biomedical applications of ribosome inactivating proteins (RIPs): from bioconjugate to nanoconstructs, J. Biomed. Sci. 23 (2016) 54–61.
[17] R. Gilabert-Oriol, A. Weng, B. Mallinckrodt, M.F. Melzig, H. Fuchs, M. Thakur, Immunotoxins constructed with ribosome-inactivating proteins and their enhancers: a lethal cocktail with tumor specific efficacy, Curr. Pharm. Des. 20 (2014) 6584–6643.
[18] S. Stahl, F. Mueller, I. Pastan, U. Brinkmann, Factors that determine sensitivity and resistances of tumor cells towards antibody-targeted protein toxins, in: R.S. Verma, B. Bonavida (Eds.), Resistance to Immunotoxins in Cancer Therapy, Springer International Publishing, Cham, 2015, pp. 57–73.
[19] E.D. Deeks, J.P. Cook, P.J. Day, D.C. Smith, L.M. Roberts, J.M. Lord, The low lysine content of ricin A chain reduces the risk of proteolytic degradation after translocation from the endoplasmic reticulum to the cytosol, Biochemistry 41 (2002) 3405–3413.
[20] S. Santanche, A. Bellelli, M. Brunori, The unusual stability of saporin, a candidate for the synthesis of immunotoxins, Biochem. Biophys. Res. Commun. 234 (1997) 129–132.
[21] Y. Endo, K. Tsurugi, RNA N-glycosidase activity of ricin A-chain. Mechanism of action of the toxic lectin ricin on eukaryotic ribosomes, J. Biol. Chem. 262 (1987) 8128–8130.
[22] L. Barbieri, M.G. Battelli, F. Stirpe, Ribosome-inactivating proteins from plants, Biochim. Biophys. Acta 1154 (1993) 237–282.
[23] M. Puri, I. Kaur, M.A. Perugini, R.C. Gupta, Ribosome-inactivating proteins: current status and biomedical applications, Drug Discov. Today 17 (2012) 774–783.
[24] A. Di Maro, L. Citores, R. Russo, R. Iglesias, J.M. Ferreras, Sequence comparison and phylogenetic analysis by the maximum likelihood method of ribosome-inactivating proteins from angiosperms, Plant Mol. Biol. 85 (2014) 575–588.
[25] F. Stirpe, M.G. Battelli, Ribosome-inactivating proteins: progress and problems, Cell. Mol. Life Sci. 63 (2006) 1850–1866.
[26] S.-W. Park, R. Vepachedu, N. Sharma, J.M. Vivanco, Ribosome-inactivating proteins in plant biology, Planta 219 (2004) 1093–1096.
[27] O. Akkouh, T.B. Ng, R.C. Cheung, J.H. Wong, W. Pan, C.C. Ng, O. Sha, P.C. Shaw, W.Y. Chan, Biological activities of ribosome-inactivating proteins and their possible applications as antimicrobial, anticancer, and anti-pest agents and in neuroscience research, Appl. Microbiol. Biotechnol. 99 (2015) 9847–9863.
[28] R. Vago, C.J. Marsden, J.M. Lord, R. Ippoliti, D.J. Flavell, S.U. Flavell, A. Ceriotti, M.S. Fabbrini, Saporin and ricin A chain follow different intracellular routes to enter the cytosol of intoxicated cells, FEBS J. 272 (2005) 4983–4995.
[29] M. de Virgilio, A. Lombardi, R. Caliandro, M.S. Fabbrini, Ribosome-inactivating proteins: from plant defense to tumor attack, Toxins (Basel) 2 (2010) 2699–2737.
[30] L. Barbieri, M. Ciani, T. Girbes, W.Y. Liu, E.J. Van Damme, W.J. Peumans, F. Stirpe, Enzymatic activity of toxic and non-toxic type 2 ribosome-inactivating proteins, FEBS Lett. 563 (2004) 219–222.
[31] R. Tamburino, E. Pizzo, C. Sarcinelli, E. Poerio, F. Tedeschi, A.G. Ficca, A. Parente, A. Di Maro, Enhanced cytotoxic activity of a bifunctional chimeric protein containing a type 1 ribosome-inactivating protein and a serine protease inhibitor, Biochimie 94 (2012) 1990–1996.
[32] A. Di Maro, P. Valbonesi, A. Bolognesi, F. Stirpe, P. De Luca, G. Siniscalco Gigliano, L. Gaudio, P. Delli Bovi, P. Ferranti, A. Malorni, A. Parente, Isolation and characterization of four type-1 ribosome-inactivating proteins, with polynucleotide:adenosine glycosidase activity, from leaves of *Phytolacca dioica* L, Planta 208 (1999) 125–131.
[33] E. Poerio, S. Di Gennaro, A. Di Maro, F. Farisei, P. Ferranti, A. Parente, Primary structure and reactive site of a novel wheat proteinase inhibitor of subtilisin and chymotrypsin, Biol. Chem. 384 (2003) 295–304.
[34] V. Sgambati, E. Pizzo, M.C. Mezzacapo, A.M. Di Giuseppe, N. Landi, E. Poerio, A. Di Maro, Cytotoxic activity of chimeric protein PD-L4UWSCI$^{(tr)}$ does not appear be affected by specificity of inhibition mediated by anti-protease WSCI domain, Biochimie 107 Pt B (2014) 385–390.

[35] A.B. Hendrich, K. Michalak, Lipids as a target for drugs modulating multidrug resistance of cancer cells, Curr. Drug Targets 4 (2003) 23–30.
[36] F. Mollinedo, C. Gajate, Lipid rafts as major platforms for signaling regulation in cancer, Adv. Biol. Regul. 57 (2015) 130–146.
[37] D. Kullenberg, L.A. Taylor, M. Schneider, U. Massing, Health effects of dietary phospholipids, Lipids Health Dis. 11 (2012) 3–18.
[38] F. Del Vecchio Blanco, V. Cafaro, A. Di Maro, R. Scognamiglio, G. Siniscalco, A. Parente, A. Di Donato, A recombinant ribosome-inactivating protein from the plant *Phytolacca dioica* L. produced from a synthetic gene, FEBS Lett. 437 (1998) 241–245.
[39] R. Iglesias, L. Citores, S. Ragucci, R. Russo, A. Di Maro, J.M. Ferreras, Biological and antipathogenic activities of ribosome-inactivating proteins from *Phytolacca dioica* L, Biochim. Biophys. Acta 1860 (2016) 1256–1264.
[40] L. Whitmore, B.A. Wallace, Protein secondary structure analyses from circular dichroism spectroscopy: methods and reference databases, Biopolymers 89 (2008) 392–400.
[41] L.M. Pavone, P. Del Vecchio, P. Mallardo, F. Altieri, V. De Pasquale, S. Rea, N.M. Martucci, C.S. Di Stadio, P. Pucci, A. Flagiello, M. Masullo, P. Arcari, E. Rippa, Structural characterization and biological properties of human gastrokine 1, Mol. BioSyst. 9 (2013) 412–421.
[42] C.N. Pace, Determination and analysis of urea and guanidine hydrochloride denaturation curves, Methods Enzymol. 131 (1986) 266–280.
[43] R. Oliva, P. Del Vecchio, M.I. Stellato, A.M. D'Ursi, G. D'Errico, L. Paduano, L. Petraccone, A thermodynamic signature of lipid segregation in biomembranes induced by a short peptide derived from glycoprotein gp36 of feline immunodeficiency virus, Biochim. Biophys. Acta 1848 (2015) 510–517.
[44] R. Del Giudice, A. Arciello, F. Itri, A. Merlino, M. Monti, M. Buonanno, A. Penco, D. Canetti, G. Petruk, S.M. Monti, A. Relini, P. Pucci, R. Piccoli, D.M. Monti, Protein conformational perturbations in hereditary amyloidosis: differential impact of single point mutations in ApoAI amyloidogenic variants, Biochim. Biophys. Acta 1860 (2016) 434–444.
[45] A. Ruggiero, A. Chambery, A. Di Maro, A. Parente, R. Berisio, Atomic resolution (1.1 A) structure of the ribosome-inactivating protein PD-L4 from *Phytolacca dioica* L. leaves, Proteins 71 (2008) 8–15.
[46] A.M. Facchiano, S. Costantini, A. Di Maro, D. Panichi, A. Chambery, A. Parente, S. Di Gennaro, E. Poerio, Modeling the 3D structure of wheat subtilisin/chymotrypsin inhibitor (WSCI). Probing the reactive site with two susceptible proteinases by time-course analysis and molecular dynamics simulations, Biol. Chem. 387 (2006) 931–940.
[47] G. Fiorentino, I. Del Giudice, L. Petraccone, S. Bartolucci, P. Del Vecchio, Conformational stability and ligand binding properties of BldR, a member of the MarR family, from *Sulfolobus solfataricus*, Biochim. Biophys. Acta 1844 (2014) 1167–1172.
[48] O. Canadas, C. Casals, Differential scanning calorimetry of protein-lipid interactions, Methods Mol. Biol. 974 (2013) 55–71.